

# Coherent Time-Delayed Atom-Light Interferometer

G. Campbell, M. Hosseini, B. M. Sparkes, P. K. Lam and B. C. Buchler

*Centre for Quantum Computation and Communication Technology,*

*Department of Quantum Science, The Australian National University, Canberra, Australia*

(Dated: March 2, 2022)

We present experimental observations of interference between an atomic spin coherence and an optical field in a  $\Lambda$ -type gradient echo memory. The interference is mediated by a strong classical field that couples a weak probe field to the atomic spin coherence through a resonant Raman transition. Interference can be observed between a prepared spin coherence and another propagating optical field, or between multiple  $\Lambda$  transitions driving a single spin coherence. In principle, the interference in each scheme can yield a near unity visibility and could be used as a coherent all-optical switch.

PACS numbers: 42.50.Gy, 42.50.Hz

Coherent manipulation of atomic systems using photons is a key element of many quantum atom-optics experiments. The ability to controllably tune atom-light interactions while preserving the quantum properties of a system also has great potential with regard to the development of quantum information technology. Many of the techniques employed in quantum atom-optics involve interaction of light with ensembles of atoms that have long-lived coherences between hyperfine energy levels. In such systems, a two-photon transition between hyperfine states can be used to manipulate the atomic state in a coherent manner. Examples of this include stimulated Raman adiabatic passage (STIRAP) [1], electromagnetically induced transparency (EIT) [1, 2] and photon echoes [3, 4], all of which have been proposed as central elements in a range of protocols for storing and processing optical quantum information.

Within the range of schemes that exploit light-atom interactions, a number of them, particularly photon echo schemes, pertain to interference effects between the quantum modes. A time-delayed quantum interferometer has previously been proposed as a method for quantum interference between two single photons [5]. Experimental observation of interference between backward-propagating stimulated photon echoes has also been reported [3], where two echoes have been selectively chosen in time to destructively interfere while the information contained in the suppressed echo was not recovered from the sample. Furthermore, the phase preserving nature of storage was previously investigated by interfering echoes generated from separate optical memories [6].

In this paper, we investigate the coherent interference of atomic polarisation and an optical field using the three-level gradient echo memory ( $\Lambda$ -GEM) technique [7–10]. We treat the read and write stages of the memory as being analogous to a beam-splitting operation acting between an optical mode and an atomic spin coherence. Both the splitting ratio and the interference phase are controlled optically via the strength of the Raman coupling field.

We explore the nature of the atom-light coupling through two separate mechanisms. The first scheme (Fig. 1(a)) is a time-domain interferometer. We pre-

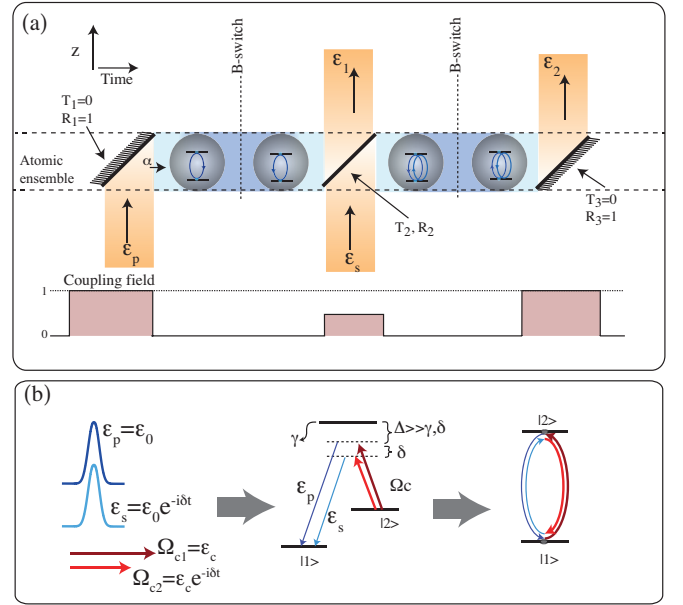


FIG. 1: (a) Schematic representation of atom-light interference in the memory. The probe pulse,  $\mathcal{E}_p^n$ , is fully absorbed in the atomic coherence ( $\alpha$ ). The second steering pulse,  $\mathcal{E}_s$ , enters the memory at the precise time that the first echo is being emitted so that it can interfere with the recalled light. The interference is determined by relative phase of the pulses and the effective beamsplitter ( $T_2, R_2$ ), which is fully controlled by the strength of the Raman coupling field. The remaining atomic polarisation can be recalled later as  $\mathcal{E}_2$ . (b) Double- $\Lambda$  schematic level structure for the optical fields used for quantum interference of two Raman absorption paths of signal fields (probe and steering) with different frequencies.

pare the atomic polarisation by storing a pulse of light in the atomic memory. A second steering pulse is sent into the memory just as the stored field is being recalled. The two pulses are observed to interfere as polaritonic modes. The second scheme (Fig. 1(b)) is a frequency domain interferometer. In this case the atomic coherence is simultaneously driven via two distinct Raman transitions. Interference is then produced between the two nondegenerate absorption paths. We first briefly intro-

duce the storage technique in general and then explain each scheme in more detail.

The  $\Lambda$ -GEM technique operates by applying a linearly varying detuning to an ensemble of three-level atoms. A strong coupling field is then used to couple a weak probe field to the long-lived atomic spin coherence, which dephases due to the applied magnetic field gradient. By reversing the sign of the gradient, the atomic dipoles can be rephased, resulting in a photon echo. It has been shown previously that  $\Lambda$ -GEM is capable of efficient and noiseless storage of quantum states of light [9, 10]. Moreover, this scheme has the capacity to arbitrarily access the multiple stored bits of information [8] and manipulated the stored information in the time and frequency domains [11].

The behaviour of the  $\Lambda$ -GEM is best understood using a spatial Fourier decomposition of the optical field  $\hat{\mathcal{E}}(t, k)$  and atomic field  $\sigma_{12}(t, k)$ . The normal mode of the  $\Lambda$ -GEM is defined as  $\hat{\psi}(t, k) = k\hat{\mathcal{E}}(t, k) + N\frac{\Omega_c}{\Delta}\sigma_{12}(t, k)$  and propagates in the  $(t, k)$  plane following the equation [12]

$$\left( \frac{\partial}{\partial t} - \eta(t) \frac{\partial}{\partial k} - i \frac{gN\Omega_c^2}{k\Delta^2} \right) \hat{\psi}(t, k) = 0, \quad (1)$$

where  $N$  is the linear atomic density,  $g$  is the atom-light coupling,  $\Omega_c$  is the coupling field Rabi frequency,  $\Delta$  is the Raman detuning from the excited states, and  $\eta(t)$  is slope of the gradient magnetic field that can vary in time. Like the normal mode in EIT[2],  $\hat{\psi}(t, k)$  is a combination of atomic polarisation and optical field and can be considered a polariton. In  $\Lambda$ -GEM, however, the normal mode is defined in the spatial Fourier domain. The degree to which the ground state coherence has dephased is described by the polariton's position in  $k$ -space. The velocity at which the polariton propagates in the  $k$ -direction is proportional to the frequency gradient.

The propagation of the  $\Lambda$ -GEM polariton in  $k$ -space can be controlled through the gradient magnetic field. An optical pulse entering the medium will create a polariton at  $k = 0$ , which then evolves in  $k$  values. By switching the sign of the magnetic field gradient, the evolution of the polariton is reversed. When the polariton again reaches  $k = 0$  the atomic coherence is rephased and the polariton is recalled as an optical field, provided that the coupling field is present.

Our first experiment investigates interference of light pulses with a mode stored in the atomic memory. Following on from Ref. [13], this effect can be thought of as a time-delayed beamsplitter system. The effective optical depth (OD) of a  $\Lambda$ -GEM is defined as

$$\beta = \frac{gN}{\eta} \left( \frac{\Omega_c}{\Delta} \right)^2. \quad (2)$$

For the writing stage the transmissivity,  $T(\beta)$ , of the effective beamsplitter is the fraction of the input light that is leaked through the memory so that  $T(\beta) = e^{-2\pi\beta}$ , while the fraction of the light written into the memory is given by the reflectivity  $R(\beta) = 1 - T(\beta)$ . For the

reading stage, the  $R(\beta)$  will be the fraction of  $\psi$  that is converted into a recalled optical field while  $T(\beta)$  will be the fraction that remains in the memory. Since  $T(\beta)$  and  $R(\beta)$  are defined by the strength of the coupling field, one can fully tune the transmissivity of the beam-splitting through the power of the coupling field. A series of reading and writing events, as shown in Fig. 1(a), can then be described using appropriate reflectivities. The amount of light recalled in the first echo is given by  $\mathcal{E}_1 = \sqrt{R_1 R_2} e^{-\gamma_0 \tau} \mathcal{E}_p + e^{i\theta} \sqrt{T_2} \mathcal{E}_s$  where the exponential term arises from the decay of  $\mathcal{E}_p$  during the storage time  $\tau$  and the phase  $\theta$  can be chosen at will. This equation shows that interference can arise between recalled fraction of  $\mathcal{E}_p$  and  $\mathcal{E}_s$  and, in particular, if  $\sqrt{R_1 R_2} e^{-\gamma_0 \tau} = \sqrt{T_2}$  and  $\theta = \pi$  then  $\mathcal{E}_1$  can be fully suppressed. We have ignored details in this qualitative analysis. In particular, the temporal modes of the pulses have to be matched to observe strong interference. Factors that limit ideal interference will be discussed later when we analyse the results of our experiments.

Figure 2 shows a numerical simulation of this interference scheme using the methods described in [12]. The simulation shows the evolution of the electric field in real space (the  $z - t$  plane) and the atomic spin coherence in Fourier-space (the  $k - t$  plane). In this numerical simulation the atomic and electric fields are out of phase. This results in a suppression of the echo from the first pulse. The constructively interfered atomic polarisation is recalled in field  $\mathcal{E}_2$  after the second gradient switch.

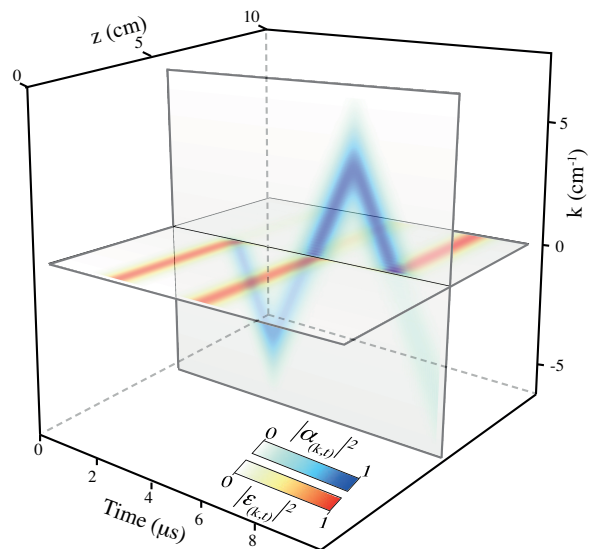


FIG. 2: Numerical simulation showing interference between electric field, plotted on the  $z$ - $t$  plane, and atomic excitations, plotted on the  $k$ - $t$  plane, where the second light pulse is out of phase from the first echo field. The parameters used in the simulations are:  $gNL/\gamma = 40$ ,  $\Omega_c/\Delta = 0.75$ ,  $\Omega_c(t = 4\mu s) = 0.7\Omega_c(t = 2\mu s)$  and  $\phi_{\mathcal{E}_s} - \phi_{\mathcal{E}_p} = \pi$

The experiment was performed using an ensemble of warm  $^{87}\text{Rb}$  atoms and a linear switchable varying magnetic field [9]. As described, we stored a probe pulse

in the memory and injected the steering pulse just as the atomic polarisation excited by the probe returned to  $k = 0$ . The recalled pulses  $\mathcal{E}_1$  and  $\mathcal{E}_2$  were then measured as a function of the relative phase of the probe and steering pulses. The phase of the atomic polarisation depends on the relative phase of the coupling and probe fields. It is therefore possible to modulate the phase of the interference by scanning the phase of either the steering pulse or the corresponding coupling field. Fig. 3(a) shows interference fringes for  $\mathcal{E}_1$  (blue, dashed line) and  $\mathcal{E}_2$  (red, solid line) obtained by varying the phase of the coupling field corresponding to the steering pulse. In these data the coupling field power and steering pulse power were tuned to find the maximum fringe visibility on  $\mathcal{E}_2$ , which was found to be 68%. The visibility of  $\mathcal{E}_1$  echo is, in this case, substantially lower due to the power mismatch of the steering pulse and the recalled atomic polarisation required to optimise the interference in  $\mathcal{E}_2$ .

Control over the effective beamsplitter ratio is demonstrated in Fig. 3 (b). It can be seen that by varying the coupling field power the effective splitting ratio can be tuned to find a maximum in the interference. It is interesting to note that for strong coupling fields, one optical pulse is written into memory while another is being recalled with little interference between the two, analogous to a high-reflectivity beamsplitter. For a weak coupling field, on the other hand, the effective beamsplitter becomes fully transmissive, again meaning no interference between the pulses as the steering pulse passes straight through without storage and the probe pulse remains trapped in the atomic polarisation.

Now we consider the second experiment, in which the interference results from driving a single atomic coherence with multiple two-photon transitions as depicted in Fig. 1(b). The essence of interference in this case is very similar to the previous setup, however here the interference happens between two pulses with frequencies separated by  $\delta$  entering the medium at the same time and interacting with the atoms through the use of two coupling fields,  $\Omega_{C1}$  and  $\Omega_{C2}$ . This method is similar to multimode EIT experiments [14, 15], in which a particular superposition of frequency modes is coupled to an atomic coherence via a Raman transition. Unlike EIT, however, the optical modes which are not coupled to the atomic coherence in the  $\Lambda$ -GEM scheme propagate through the atomic medium with little loss.

To experimentally observe double-Raman interference, we stored probe and steering pulses with different frequencies via two coupling fields to a single atomic coherence. The frequency difference between the probe and steering fields was set to 1 MHz, which was larger than the memory bandwidth of 300 kHz to avoid overlap between two broadened Raman lines. In the far-detuning and adiabatic regimes, this double- $\Lambda$  system is equivalent to a quasi-two-level system interacting with two fields of different Rabi frequency (see Fig. 1 (b)). The interference between the two  $\Lambda$  transitions will change the response of the medium to the probe and steering

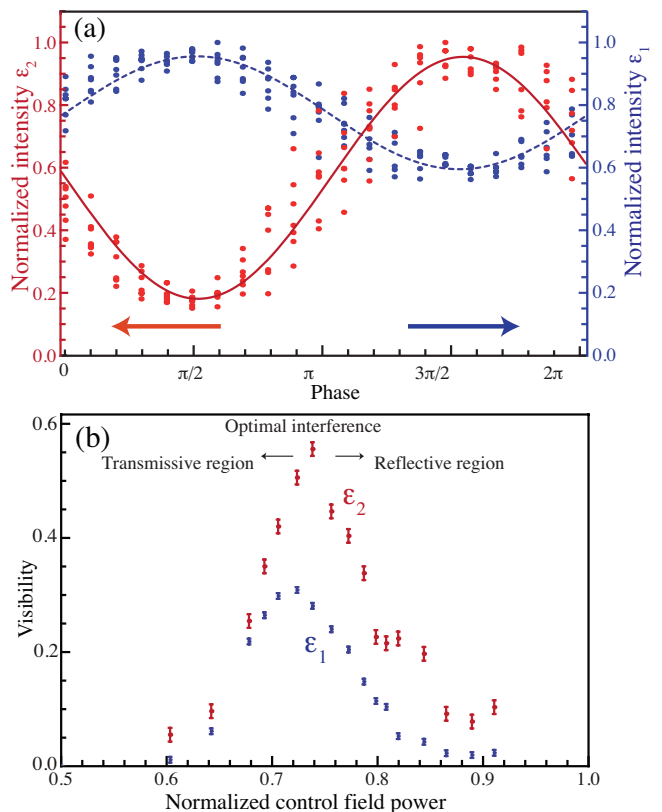


FIG. 3: (a) Atom-light interference fringes at different times resulted from interaction of the steering pulse with echo generated from the probe pulse. The first arm of the interferometer which is in the optical mode leaves the memory (blue data) and the second arm is stored as an atomic coherence that is transformed back to the light field after re-switching the B-field (red data). These data were taken by optimising the experimental parameters such as efficiency. The dashed blue and solid red lines are sinusoidal fits to the corresponding data. The red and blue data yield a fringe visibility of 68% and 23%, respectively. (b) Visibility of fringes for two pulses separated in time at the first (blue points) and second (red points) reading stage as a function of the normalised coupling field power.

pulses. When they destructively interfere, the absorption of the probe and steering fields can be suppressed and both pulses are transmitted through the medium. When the two  $\Lambda$  transitions are in-phase, both pulses are coherently absorbed and can be recalled later on-demand. Fig. 4 shows the interference fringe obtained by varying the relative phase between the two Raman absorption lines. This was done by sweeping the phase of one of the coupling fields while it is on the Raman resonance frequency.

In both the time and frequency domain interference experiments we attribute the less-than-unity fringe visibility primarily to spatial and temporal mode mismatch between the probe polariton and the steering pulse. We believe that this is mainly due to the atomic motion and non-zero transverse magnetic field, which affects the echo

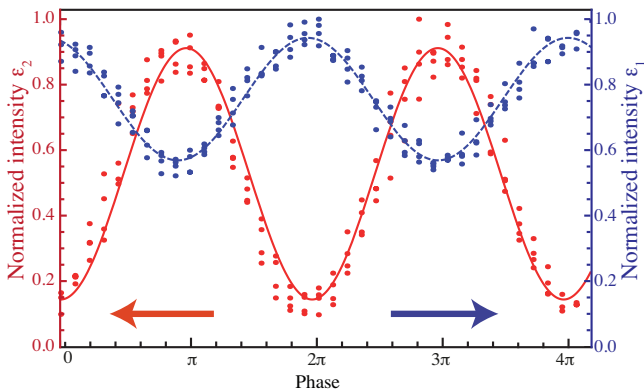


FIG. 4: Interference fringes from transmitted (blue) and absorbed (red) part of light resulted from interference between double- $\Lambda$  transitions created from the probe and steering pulses of different frequency stored simultaneously in the memory. The dashed blue and solid red lines are sinusoidal fits to the corresponding data. The red and blue data yield a fringe visibility of 73% and 25%, respectively.

signal for long storage times. This can be justified by larger visibility measured in the frequency-domain interference scheme, where interference occurs between pulses simultaneously interact with the atomic coherence. During the storage time, atomic diffusion can change the spatial mode of the coherence and as a result, the echo signal will have a slightly different mode compare to the input signal. This effect is negligible for shorter storage times. The presence of a transverse magnetic field can induce an extra spatial frequency ( $k_x$  and  $k_y$ ) during storage. The transverse  $k$  vector is imprinted to the echo signal at the readout diverting the output optical field slightly com-

pare to the steering pulse. In the beamsplitter analogy, this amounts to a poorly aligned interferometer. An inhomogeneous longitudinal magnetic field can alter the shape of the echo signal compared to its input leading to temporal mode mismatch. We anticipate, therefore, that the visibility could be improved by increasing the buffer gas pressure or using cold atomic sample in order to increase the time of flight of the atoms and taking extra care with the magnetic environment to prevent pulse deflection and distortion. Numerical simulation reveals that, in limits of large OD, interference visibility of the system can approach unity.

In summary, we have demonstrated interference effects between propagating optical fields and a collective atomic spin coherence. Fringe visibilities of 68% and 73% were observed for time-domain and frequency-domain interference schemes, respectively. These schemes may have relevance to manipulating optical quantum information. Unlike previous schemes, interference in a gradient echo memory could offer dynamic, optically addressable linear operations on optical qubits with little loss. These gates could operate on either time-bin or frequency multiplexed qubits or even a combination thereof. The time-delayed beamsplitter scheme can also be used for optical quantum state engineering [16, 17] and also for optimal Gaussian purification of coherent states from several imperfect copies [18]. The ability to construct this type of interferometer is also of interest in building a coherent all-optical switch [19–21].

This research was conducted by the Australian Research Council Centre of Excellence for Quantum Computation and Communication Technology (project number CE110001027).

- 
- [1] M. Fleischhauer, A. Imamoglu, and J. P. Marangos, *Rev. Mod. Phys.* **77**, 633 (2005).
  - [2] M. Fleischhauer and M. D. Lukin, *Phys. Rev. Lett.* **84**, 5094 (2000).
  - [3] M. Arend, E. Bloch, and S. R. Hartmann, *Opt. Lett.* **18**, 1789 (1993).
  - [4] M. Arend, E. Bloch, and S. R. Hartmann, *Opt. Exp.* **18**, 1789 (1993).
  - [5] S. A. Moiseev, *Quant. Elect.* **31**, 557 (2001).
  - [6] M. U. Staudt and et. al., *Phys. Rev. Lett.* **99**, 173602 (2007).
  - [7] G. Hétet, M. Hosseini, B. M. Sparkes, D. Oblak, P. K. Lam, and B. C. Buchler, *Opt. Lett.* **33**, 2323 (2008).
  - [8] M. Hosseini, B. M. Sparkes, G. Hetet, J. J. Longdell, P. K. Lam, and B. C. Buchler, *Nature* **461**, 241 (2009).
  - [9] M. Hosseini, B. M. Sparkes, G. Campbell, P. K. Lam, and B. C. Buchler, *Nat. Commun.* **2** (2011).
  - [10] M. Hosseini, G. Campbell, B. M. Sparkes, P. K. Lam, and B. C. Buchler, *Nat. Phys.*, DOI: 10.1038/NPHYS2021 (2011).
  - [11] B. C. Buchler, M. Hosseini, G. Hetet, B. M. Sparkes, and P. K. Lam, *Opt. Lett.* **35**, 1091 (2010).
  - [12] G. Hetet, J. J. Longdell, M. J. Sellars, P. K. Lam, and B. C. Buchler, *Phys. Rev. Lett.* **101**, 203601 (2008).
  - [13] J. J. Longdell, G. Hetet, P. K. Lam, and M. J. Sellars, *Phys. Rev. A* **78**, 032337 (2008).
  - [14] J. Appel, E. Figueroa, and A. Lvovsky, *Opt. Lett.* **32**, 2771 (2007).
  - [15] G. Campbell, A. Ordog, and A. I. Lvovsky, *New J. of Phys.* **11**, 106021 (2009).
  - [16] E. Bimbard, N. Jain, A. MacRae, and A. I. Lvovsky, *Nat. Phot.* **4**, 243 (2010).
  - [17] W. Tittel, J. Brendel, H. Zbinden, and N. Gisin, *Phys. Rev. Lett.* **84**, 4737 (2000).
  - [18] U. L. Andersen, R. Filip, J. Fiurásek, V. Josse, and G. Leuchs, *Phys. Rev. A* **72**, 060301(R) (2005).
  - [19] S. E. Harris and Y. Yamamoto, *Phys. Rev. Lett.* **81**, 3611 (1998).
  - [20] J.-H. Wu, J.-Y. Gao, J.-H. Xu, L. Silvestri, M. Artoni, G. C. La Rocca, and F. Bassani, *Phys. Rev. Lett.* **95**, 057401 (2005).
  - [21] H. Schmidt and R. J. Ram, *App. Phys. Lett.* **76**, 3173 (2000).